

Elsevier Editorial System(tm) for Nuclear Inst. and Methods in Physics Research, A

Manuscript Draft

Manuscript Number:

Title: Performance of irradiated n⁺-on-p silicon microstrip sensors

Article Type: Research Paper

Section/Category: High Energy Physics Detectors

Keywords: silicon microstrip detector; charge collection; irradiation; p⁺ bulk

Corresponding Author: Dr Kazuhiko HARA, PhD

Corresponding Author's Institution: School of Pure and Applied Sciences

First Author: Kazuhiko HARA, PhD

Order of Authors: Kazuhiko HARA, PhD

Manuscript Region of Origin:

Abstract: The silicon microstrip detector type with n⁺-on-p readout fabricated on p⁺ bulk, n⁺-on-p, is a candidate to be operational in radiation environments much severer than in LHC. We characterized n⁺-on-p detectors which were irradiated up to 1.1 $\times 10^{14}$ protons/cm² ten years ago. The noise level and charge collection were evaluated using the ATLAS SCT readout electronics system. Radiation-induced increase in the noise and loss in the charge collection are not significant. The charge collection is not degraded in any particular point in the inter-strip region when the detector is operated under partial depletion.

3 April 2006

Performance of irradiated n^+ -on- p silicon microstrip sensors

K. Hara^a, A. Mochizuki^a, T. Munakata^a, Y. Nakamura^a,
K. Nakamura^a, K. Inoue^a, Y. Ikegami^b, T. Kohriki^b,
S. Terada^b, Y. Unno^b

^a *Institute of Pure and Applied Sciences, University of Tsukuba, 1-1-1 Ten'nodai, Tsukuba, Ibaraki 305-8571, Japan*

^b *High Energy Accelerator Research Organization (KEK), Oho 1-1, Tsukuba, Ibaraki 305-0801, Japan*

Abstract

The silicon microstrip detector type with n^+ readout fabricated on p bulk, n^+ -on- p , is a candidate to be operational in radiation environments much severer than in LHC. We characterized n^+ -on- p detectors which were irradiated up to 1.1×10^{14} protons/cm² ten years ago. The noise level and charge collection were evaluated using the ATLAS SCT readout electronics system. Radiation-induced increase in the noise and loss in the charge collection are not significant. The charge collection is not degraded in any particular point in the inter-strip region when the detector is operated under partial depletion.

Key words: silicon microstrip detector; charge collection; irradiation; p bulk

1 Introduction

Silicon microstrip detectors have become one of the common apparatus in high energy physics experiments for tracking in a region close to the interaction point or even in the entire "inner" tracking volume. The advantages of silicon detectors are, among many others, superior spatial resolution and resistance against radiation if they are designed properly. The two large silicon microstrip detector systems of ATLAS [1] and CMS [2] groups at LHC employ a scheme of p^+ readout strips fabricated in n bulk, or p^+ -on- n . These detectors are expected to remain as precision trackers up to the fluence of 2×10^{14} n_{eq} cm⁻² anticipated for 10 years of LHC operation. The bulk will behave as p type by radiation damage and then the full depletion voltage increases with fluence.

Since the inverted p^+ -on- p detector needs to be fully depleted to electrically isolate the readout strips, the detector lifetime is determined by the high voltage applicable to the detector. Efficient cooling system is also essential to suppress the radiation induced leak current and to inhibit the reverse annealing to turn on.

The ATLAS SCT (semiconductor tracker) group has specified the high voltage of 350-500 V be applicable to the detector modules, depending on their radial positions from the interaction point. In the super LHC environment where the radiation becomes 10-fold severer, the high voltage would reach a few kV if we employ the same p^+ -on- n sensors. Our recent experience [3] shows that Hamamatsu Photonics can fabricate high voltage resistant detectors but to about 800 V, which is still far below the above requirement.

The n^+ -on- n detectors presently employed for ATLAS and CMS Pixel devices have longer lifetime. The signal will be read out from the junction side after the bulk inversion, which allows the sensors to be operated at partial depletion once the full depletion exceeds the applicable bias voltage. With use of low noise amplifiers, such devices can be operated with a sufficient signal-to-noise ratio even for reduced amount of signal charge. Since the n^+ -on- n detector requires backside processing and hence the sensor fabrication is much expensive, it was not employed for the strip detectors.

Intensive study is being carried out for silicon detectors for the super LHC to develop radiation hard bulk material which does not show rapid increase in the full depletion voltage [4]. As for the detector type, the n^+ -on- p is attractive for the advantage the n^+ -on- n possesses and the processing is single sided. Ten years ago, we fabricated and irradiated some n^+ -on- p sensors with 12-GeV protons up to 1.1×10^{14} /cm² [5]. The leak current increase and the full depletion voltage evolution have been evaluated. The n^+ -on- p type was not selected for the current SCT because experiences with high resistive p bulk silicon had not been accumulated by that time. We re-visited the results and added new measurements including noise and charge collection evaluations.

2 Sample detectors and irradiation

The irradiation took place in July 1995 at KEK using 12-GeV protons. The details of the irradiation and the sample detectors are described in [5].

The sample detectors are n^+ -in- p single-sided microstrip detectors with dimensions of $60 \times 34 \times 0.3 \times \text{mm}^3$, fabricated by Hamamatsu Photonics. The initial full depletion voltage was typically 160 V. The n^+ readout strips of 50 μm pitch are surrounded by p -stop implants. We employed a common p -stop

structure, the ends of p -stop strips which extend the n^+ strips in length being connected together. The p -stop doping should be optimized from the two competing requirements: The doping must be high enough to isolate the strips, while too high density creates high electric fields at the p -stop boundaries lowering the detector breakdown voltage. We compared the results of two p -stop densities of 1.0 and $0.2 \times 10^{14} /\text{cm}^2$.

The samples were irradiated to 0.43 or 1.1×10^{14} protons/ cm^2 . The temperature during and 12 days after the irradiation was 10°C . Then the temperature was kept essentially to 0°C except for some periods for transportation and measurements [5]. The depletion voltages first measured 90 days after the irradiation resulted in 150 V (210–230 V) for the samples irradiated to 0.43 (1.1×10^{14} protons/ cm^2). After the measurements, the samples have been kept in a refrigerator at 0°C . Unfortunately it then lost to control the temperature due to power outages which happened typically once a year for a weekend long period.

The samples used in this study are summarized in Table 1. These sensors are glued individually to PCB frames since the pre-irradiation measurement. The bias-ring, backside contact, and three clusters of neighboring AC pads, each consisting of five consecutive strips, are wirebonded individually to the pads on the PCB frame. The pads are used to feed the voltage and measure the bulk and interstrip capacitances.

3 Results

3.1 Bulk and interstrip capacitances

The bulk capacitance between the bias-ring and the backside was measured with an LCR meter. The LCR test signal frequency was set at 1 kHz, where the impedance contribution from the bias resistors in serial is minimized. The shape of the CV curves are dependent on the temperature due to large radiation induced leak current: At lower temperatures the shape of the CV curves becomes clearer to extract the full depletion voltage V_{FD} . Figure 1 shows the CV curves measured at -20°C for the four irradiated and one non-irradiated samples. The full depletion voltages determined from these curves are 350-330 (210-230) and 200-205 (150-155) V, respectively, for the samples irradiated to 1.1 and $0.4 \times 10^{14} /\text{cm}^2$. The numbers in the parentheses are V_{FD} measured 90 days after the irradiation [5]. The non-irradiated sample has 160 (152) V. The full depletion voltage of the non-irradiated samples remains similar, but we see a tendency that the full depletion voltages have increased in the 10 years. The uncontrolled temperature rise may explain the difference, although

any qualitative estimate is not possible without the temperature record in the past ten years.

The interstrip capacitance was measured at -20°C and at 0.4 MHz LCR frequency. Among the five consecutive strips, the capacitance between the central two strips was measured with other strips set floating. The results are shown in Fig. 2. The detailed shape in the small voltage region actually depends on the temperature but the shape is hardly affected in the region above 50 V bias voltage. The interstrip capacitance drops within a few 10 V, implying that the strips are electrically isolated above that voltage. The asymptotic value at high voltages is 3.6–3.8 pF. These characteristics are not different among the irradiated and non-irradiated samples, and among the different p -stop densities.

3.2 Noise performance

The sensor noise levels were measured with a non-irradiated SCT readout chip, ABCD3T [7]. The ABCD3T, providing 128-ch binary hit data, consists of mainly amplifier-shaper-comparator chains and 132 deep digital pipeline buffers. The chip was read out using the VME-based SCTdaq system through the SCT hybrid [6]. Ten consecutive strips of each sample were wirebonded to the same channels of the same chip so that the noise affected by irradiation and p -stop doping can be directly compared.

The noise levels were evaluated in the SCT standard procedure, where the amplifier response is measured for three different test charges to extract the gain and equivalent noise charge at 1 fC threshold. The noise levels at the comparator input were measured up to 500 V bias, which is the limit specified to the sensor. For some samples, the bias was raised up to 650 V, the limit being given by the hybrid. The sample was cooled to -6 to -8°C . Figure 3 shows the results. The rms noise values are calculated from the six central channels out of the ten wirebonded channels, excluding two channels each side to suppress effects from un-bonded channels at neighbors. The mean noise distributes between 11 to 14 mV with typical rms spread among the six channels being 0.6 mV. The reproducibility of the measurement was examined for one sample by cutting the wires, re-wirebonding and repeating the measurement. The ratios averaged over six channels are found to be 0.94 to 1.00 at different bias voltages. Taking these into account, the typical uncertainty is less than 1 mV.

The irradiated samples show the results consistent within 2 mV. There is no systematic difference between the two irradiation fluences, but the un-irradiated samples show 2–3 mV larger noise especially at higher voltages above the full depletion. We see a tendency that the noise is smaller by 1 mV

for the samples with $0.2 \times 10^{14}/\text{cm}^2$ p -stop doping than $1.0 \times 10^{14}/\text{cm}^2$ doping.

3.3 Charge collection

The charge collection was evaluated by injecting Nd:YAG laser [8] of 1064 nm wavelength and about 10 ns base width. Since the laser width is shorter than the charge integration time 20 ns and the laser absorption in silicon [9] can be regarded moderate in the 0.3 mm thick bulk, this laser system can simulate the passage of charged particles. The laser intensity was adjusted to generate a signal corresponding to passage of a single high-energy charged particle. Unlike the charged particle, though, the laser is affected by sensor's local structures by additional absorption and reflection. The laser was focused to $2 \times 2 \mu\text{m}$ on the sensor surface. The response is found not to be affected by the precision of focusing: the focusing was adjusted better than $1 \mu\text{m}$ while the response changes by only 4% per $10 \mu\text{m}$ shift along the focal direction. The sensor and hybrid were placed in an aluminum box which has a window for laser injection. The box was cooled to 5°C to suppress the leakage current of the irradiated sensor.

Figure 4 shows the threshold curves of Sample H2 measured at different bias voltages. At each threshold setting 500 laser pulses were injected at 1 kHz. The number of hits is plotted in the figure as a function of the threshold voltage. Since the signal polarity of n^+ -on- p detectors is reversed, we made use of the trimming feature of the ABCD3T chip: we set the offset voltage at the discriminator (trim level) to its maximum for the discriminator works only with positive signals. Under this condition, the discriminator output turns from "1" to "0" on the presence of large negative signals out of n^+ -on- p . The ABCD3T examines the hit pattern in the three consecutive clock cycles at 40 MHz about trigger timing. We define the hit if "0" to "1" transition is present in these three clocks. Therefore, the discriminator senses the voltage in the rising part of the shaper output, e.g. the tail of the shaper output. The left part of the trapezoidal curves represents the signal pulse height distribution, the voltage at 50% efficiency corresponding to the mean pulse height. The input charge, or collected charge, is extracted from the mean pulse height minus that at zero bias, using the measured ABCD3T gain, which is typically 50 mV/fC. The collected charge for Sample H2 ($10^{14}/\text{cm}^2$ p -stop doping, $1.1 \times 10^{14}/\text{cm}^2$ irradiation) is plotted in Fig. 5. Also plotted in the figure is the data for non-irradiated sample N2 of the same p -stop doping. The collected charge increases with the bias and reaches the maximum around 130 V (300 V) for the non-irradiated (irradiated) sample, which are consistent with the full depletion voltage of 150 V (350 V). Since the maximum collected charge are consistent with each other, we can conclude that the additional charge trapping due to irradiation is little in the n^+ -on- p sensors. In a previous study, we measured

that the charge is lost by typically 10–15% for p^+ -on- n sensors irradiated to a similar radiation level [10]. We note that the charge collection at lower voltages is moderate in the n^+ -on- p sensors while substantial fraction of charge is lost in the p^+ -on- n sensors once the bias is lowered below the full depletion voltage [10].

The charge collection between the strips was measured by scanning the sensor across the strips at a step of $1\ \mu\text{m}$. Figure 6 shows the collected charges from the left and right strips separately, together with their sum (filled triangles), as a function of the distance from the left strip. The sensor is Sample H2 operated at 300 V. The sum taken at 100 V bias is also shown (open triangles) to compare the charge collection distributions at and below the full depletion. The aluminum electrodes $6\ \mu\text{m}$ wide are located at 0 and $50\ \mu\text{m}$, which are not transparent for the laser. The dips around $7\text{--}9\ \mu\text{m}$ are due to the boundary of the oxide insulators, and the dip at the center is caused by the p -stop implant $26\ \mu\text{m}$ wide. The distribution turns to be not perfectly symmetric about the center because the sensor structure itself is not symmetric due to the finite mask registration precision at sensor processing. The distributions are similar in shape for the 300 and 100 V data. This ensures that there is no particular region where the charge collection is inferior when the sensor is operated under partial depletion.

4 Summary

We have characterized n^+ -on- p sensors irradiated up to 1.1×10^{14} protons/cm² with two different p -stop doping densities of 0.2 and 1.0×10^{14} /cm². The strip isolation is achieved below 30–50 V bias voltage, the interstrip capacitance reaching 3.7 pF or 0.6 pF/cm. There is small difference between the two irradiation fluences and between the two p -stop doping densities. The noise level was found also not dependent on the fluence, while the noise for 0.2×10^{14} /cm² tends to be somewhat smaller than for 1.0×10^{14} /cm².

The collectable charge is not degraded even for the sample irradiated to 1.1×10^{14} protons/cm². The irradiated detectors can be operated below the full depletion without showing any region of inferior charge collection.

References

- [1] F. Campabadal, *et al.*, Nucl. Instrum. and Methods A 538 (2005) 384.
- [2] The Tracker Project, Technical Design Report, CERN/LHCC 98-6 CMS TDR 5 (1998): Addendum to the CMS Tracker TDR, CERN/LHC 2000-016 (2000).

- [3] T. Akimoto, *et al.*, IEEE Trans. Nucl. Sci. 51 (2004) 2215.
- [4] See, for example, F. Campabadal, *et al.* (RD50 Collaboration) CERN-LHCC-2004-031 (2005).
- [5] S. Terada, *et al.*, Nucl. Instrum. and Methods A 383 (1996) 159.
- [6] Y. Unno, *et al.*, Nucl. Instrum. and Methods A 541 (2005) 286.
- [7] W. Dabrowski, *et al.*, Proc. of 6th Workshop on Electronics for LHC Experiments, Cracow, Poland, 11–15 Sep. 2000, CERN, Geneva, 25 Oct. 2000.
- [8] K. Hara, *et al.*, Nucl. Instrum. and Methods A 541 (2005) 122; Y. Unno, *et al.*, Nucl. Instrum. and Methods A 383 (1996) 238.
- [9] A. H. Johnston, IEEE Trans. Nucl. Sci. 40-6 (1993) 1694. The absorption length from the figure in this reference is about 0.5 mm for 1064 nm infrared pulses in silicon.
- [10] T. Nakayama, *et al.*, IEEE Trans. Nucl. Sci. 47 (2000) 1885.

Table 1

The sample sensors, categorized by two p -stop doping densities, and by three radiation levels including non-irradiation.

| Sample | p -stop doping | irradiation |
|--------|------------------------------------|--------------------------------------|
| H1 | $1.0 \times 1.0^{14} /\text{cm}^2$ | $1.1 \times 10^{14} \text{ p/cm}^2$ |
| H2 | $0.2 \times 1.0^{14} /\text{cm}^2$ | $1.1 \times 10^{14} \text{ p/cm}^2$ |
| L1 | $1.0 \times 1.0^{14} /\text{cm}^2$ | $0.43 \times 10^{14} \text{ p/cm}^2$ |
| L2 | $0.2 \times 1.0^{14} /\text{cm}^2$ | $0.43 \times 10^{14} \text{ p/cm}^2$ |
| N1 | $1.0 \times 1.0^{14} /\text{cm}^2$ | not irradiated |
| N2 | $0.2 \times 1.0^{14} /\text{cm}^2$ | not irradiated |

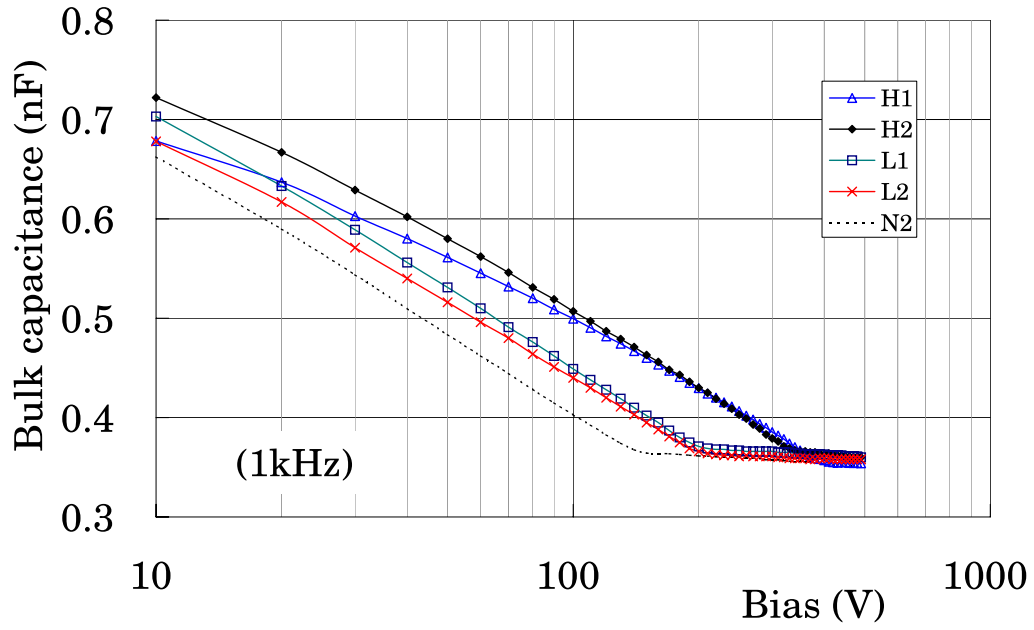


Fig. 1. Bulk capacitance (nF) as a function of the bias voltage for the four irradiated and one non-irradiated samples.

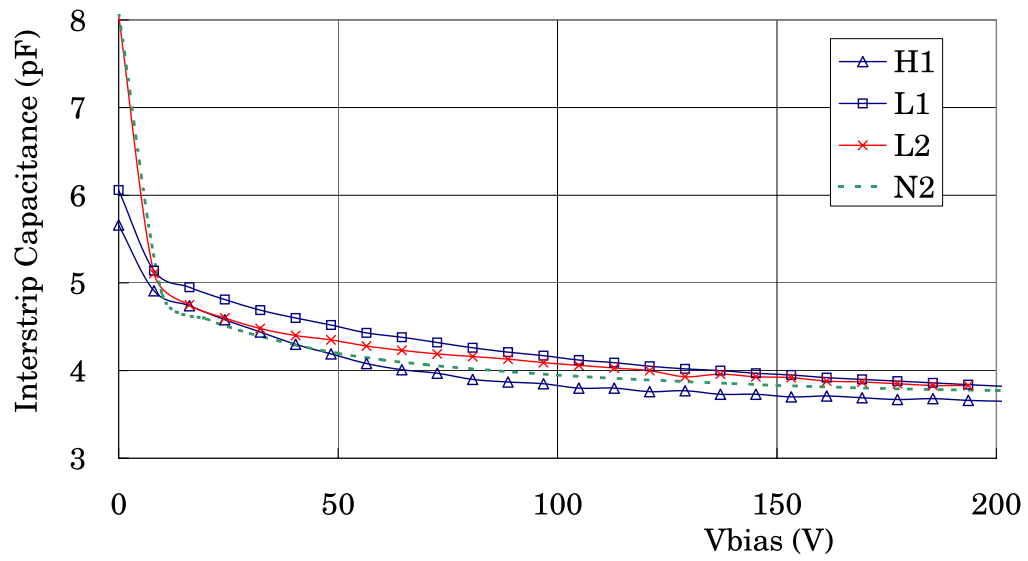


Fig. 2. Interstrip capacitance for irradiated and non-irradiated samples.

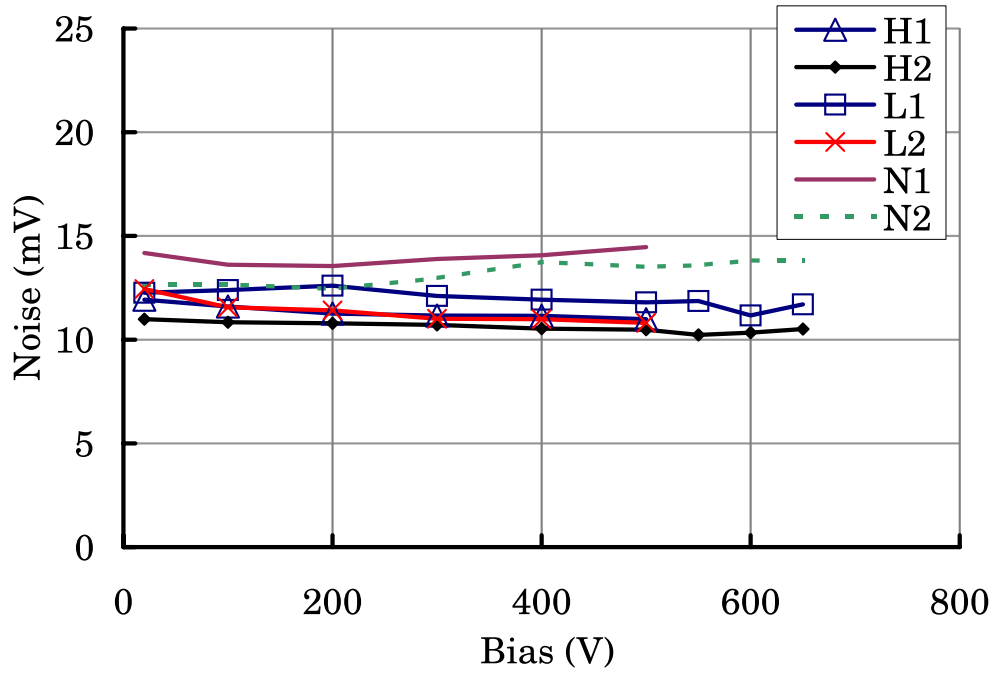


Fig. 3. The one-sigma noise levels as a function of bias voltage.

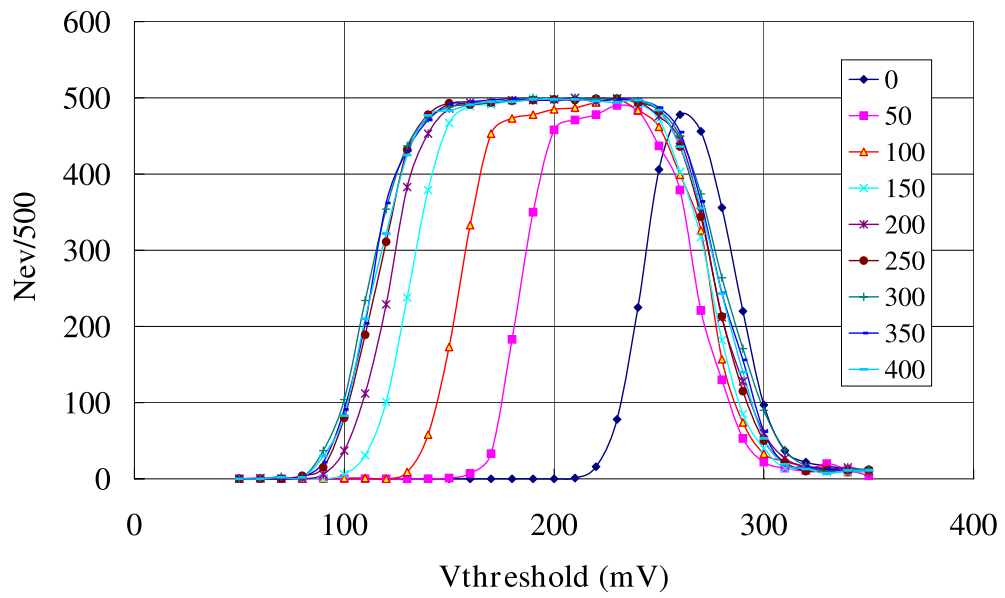


Fig. 4. Threshold curves measured at various bias voltages, 0 to 400 V.

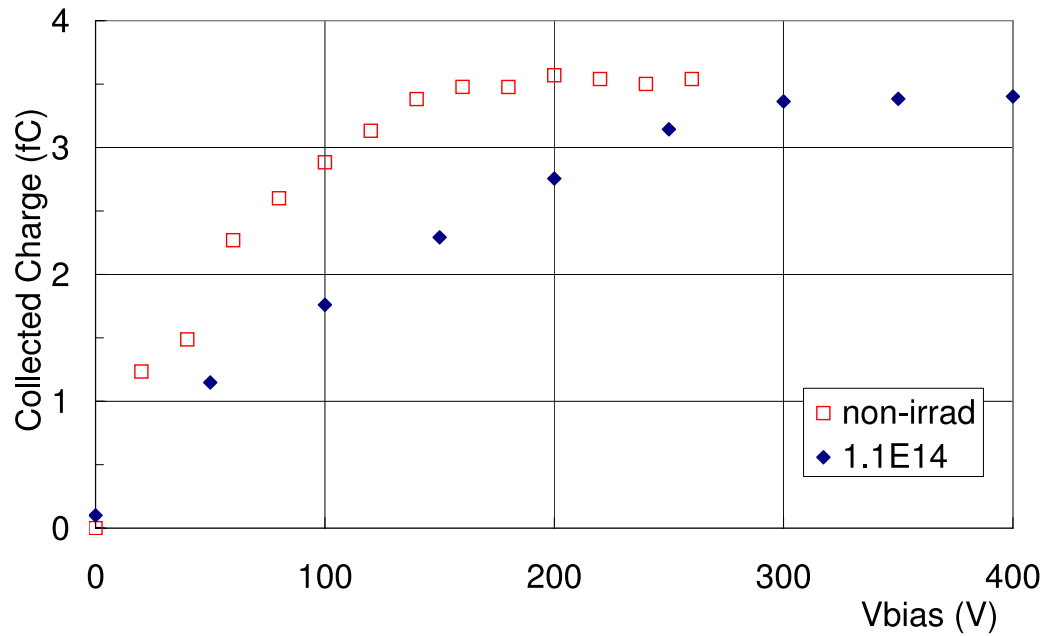


Fig. 5. Collected charge (fC) as a function of the bias voltage for (filled diamonds) irradiated Sample H2 and (open squares) non-irradiated sample N2.

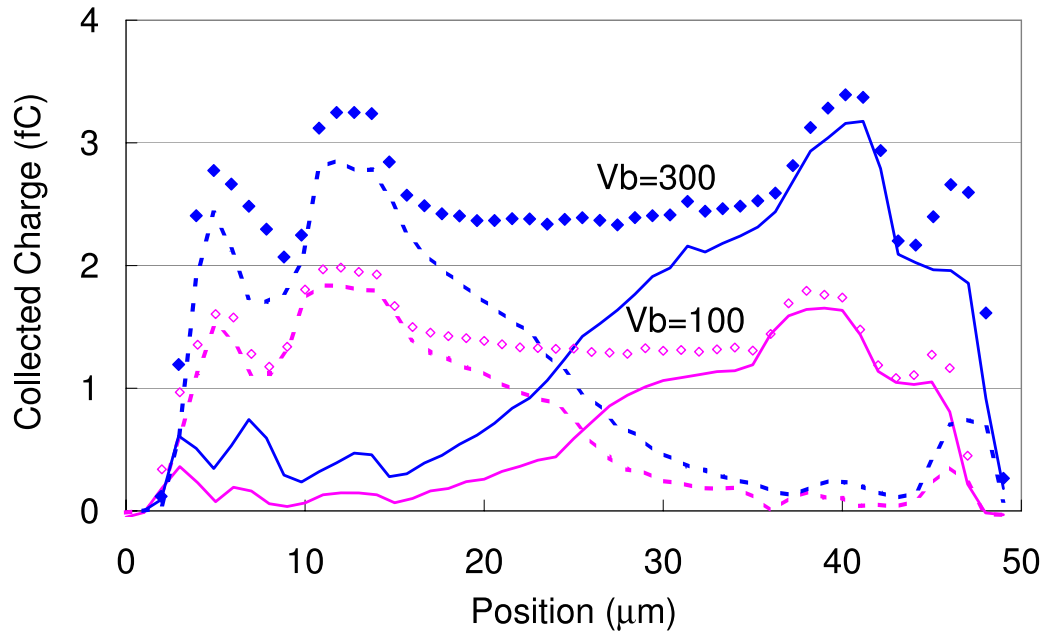


Fig. 6. Collected charge as a function of the distance from the left strip (strip pitch $50 \mu\text{m}$) for Sample H2. The charge read out from the left (right) strip is shown in dashed (solid) curves, the sum in filled diamonds for 300 V bias and in open diamonds for 100 V bias.